J. Fluid Mech. (2014), *vol.* 747, *pp.* 722–734.
doi:10.1017/jfm.2014.151

Superhydrophobic turbulent drag reduction as a function of surface grating parameters

Hyungmin Park†, Guangyi Sun‡ and Chang-Jin "CJ" Kim§

Mechanical and Aerospace Engineering Department, University of California at Los Angeles (UCLA), Los Angeles, CA 90095, USA

(Received 2 November 2013; revised 6 March 2014; accepted 13 March 2014; first published online 23 April 2014)

Despite the confirmation of slip flows and successful drag reduction (DR) in small-scaled laminar flows, the full impact of superhydrophobic (SHPo) DR remained questionable because of the sporadic and inconsistent experimental results in turbulent flows. Here we report a systematic set of bias-free reduction data obtained by measuring the skin-friction drags on a SHPo surface and a smooth surface at the same time and location in a turbulent boundary layer (TBL) flow. Each monolithic sample consists of a SHPo surface and a smooth surface suspended by flexure springs, all carved out from a 2.7×2.7 mm^2 silicon chip by photolithographic microfabrication. The flow tests allow continuous monitoring of the plastron on the SHPo surfaces, so that the DR data are genuine and consistent. A family of SHPo samples with precise profiles reveals the effects of grating parameters on turbulent DR, which was measured to be as much as ∼75 %.

Key words: drag reduction, MEMS/NEMS, turbulence control

1. Introduction

Reducing the drag of marine vehicles via gas lubrication has long been practiced by injecting gas bubbles or creating a cavitation gas pocket (Ceccio 2010) and reached a significant drag reduction (DR; ∼95 %) in a high-Reynolds-number ($Re_x \sim 10^7$) flow (Lay *et al.* 2010). Since the gas film (or bubbles) does not stay on the solid surface by nature, however, these methods should continue supplying the gas with additional energy, overshadowing the benefit of DR and limiting applications. The prospect of retaining the gas without energy input has been driving the recent explosive interest in superhydrophobic (SHPo) surfaces: a rough surface of a hydrophobic material. Surface roughness generally increases the skin-friction drag in turbulent boundary layer (TBL) flows (Jiménez 2004) except for very few specific conditions (Walsh 1982). However, if the hydrophobic roughness of the SHPo surface retains microscale air pockets and thus maintains a plastron, the resulting slip flow may bring an appreciable DR.

† Present address: Department of Mechanical & Aerospace Engineering, Seoul National University, Seoul 151-744, Korea.

‡ Present address: Institute of Robotics and Automatic Information System, Nankai University, Tianjin Key Laboratory of Intelligent Robotics, Tianjin 300071, China.

§ Email address for correspondence: cjkim@ucla.edu

Recent establishment in the slips and DRs obtained on engineered SHPo surfaces in laminar flows (Ou, Perot & Rothstein 2004; Choi & Kim 2006) have heightened the anticipation that someday an appreciable reduction can be reliably obtained in TBL flows as well (Rothstein 2010; Samaha, Tafreshi & Gad-el-Hak 2012*b*). While most SHPo surfaces in the literature were characterized simply by liquid droplets on them and not designed to produce any useful amount of slip or DR in continuous liquid flows (Bocquet & Lauga 2011), some studies started identifying and tackling the issues important to engineer drag-reducing SHPo surfaces, such as how to increase the effective slip (Lee, Choi & Kim 2008; Lee & Kim 2009) and how to maintain the plastron indefinitely, deep under water or even on a defective surface (Lee & Kim 2011, 2012).

Although a plastron-covered surface is an underlying premise for SHPo DR, the state of plastron has not been receiving proper attention in most experimental studies. Its existence has been checked only casually and its detailed state during the flow tests widely ignored. The importance has been recognized only very recently, as the plastron loss became the main roadblock against testing SHPo surfaces in turbulent flows especially in large facilities. Samaha, Tafreshi & Gad-el-Hak (2012*a*) have measured that the longevity of the plastron was shortened as the flow rate over the SHPo surface increased, and Emami *et al.* (2013) have numerically investigated the unsteady behaviour of the plastron interface by considering the diffusion of trapped air over time. They showed that the maximum hydrostatic pressure sustainable above the plastron decreases with increasing width of the water–air interface. Since the loss of plastron is inevitable in practice, Lee & Kim (2011) have developed a semi-active SHPo surface implemented with a self-regulated gas-generation mechanism, which allows indefinite plastrons.

The DR in laminar flows has been well established in recent years, as the slip is predictably related to the SHPo surface parameters (Lauga & Stone 2003; Lee *et al.* 2008). However, such a relationship has yet to be established for turbulent flows (Park, Park & Kim 2013). While the analytical, numerical and experimental results of SHPo DR converged finally for laminar flows (Lauga & Stone 2003; Ou *et al.* 2004; Choi & Kim 2006; Choi *et al.* 2006; Maynes *et al.* 2007; Woolford, Maynes & Webb 2009*a*), the studies of turbulent flows have mostly been numerical. Assuming ideal circumstances, e.g. no air loss and flat air–water interface, numerical efforts nevertheless have suggested valuable physical insights, such as the possible mechanism of turbulent DR (Min & Kim 2004; Martell, Perot & Rothstein 2009; Martell, Rothstein & Perot 2010; Busse & Sandham 2012; Park *et al.* 2013), scaling issue (Fukagata, Kasagi & Koumoutsakos 2006; Jeffs, Maynes & Webb 2010; Busse & Sandham 2012; Park *et al.* 2013) and effects of directional slip (Min & Kim 2004; Fukagata *et al.* 2006; Hasegawa, Frohnapfel & Kasagi 2011; Busse & Sandham 2012). For the mechanism of DR, Min & Kim (2004) and Park *et al.* (2013) have reported that surfaces with a streamwise slip lead to weakened near-wall turbulence structures, resulting in skin-friction DR. Martell *et al.* (2010), on the other hand, reported that SHPo surfaces do not affect the nature of near-wall turbulence structures but simply shift them toward SHPo surfaces.

With only a few experimental data in the literature (Henoch *et al.* 2006; Zhao *et al.* 2007; Daniello *et al.* 2009; Woolford *et al.* 2009*b*; Peguero & Breuer 2009; Jung & Bhushan 2010) scattered by different flow conditions, surface geometries and measurement techniques (table 1), the physics of turbulent DR on SHPo surfaces could not be investigated in earnest. To make things worse, these sporadic results have been inconsistent and unsuccessful at suggesting any trend of drag variation

https://doi.org/10.1017/jfm.2014.151 Published online by Cambridge University Press

References	Re_τ (*Re* from Refs.)	Flow geometry	SHPo surface structure	Measurement method	Maximum DR
Henoch *et al.* (2006)	150 ($Re_x = 4.1 \times 10^5$)	TBL flow	Nanoposts	Proximity sensor	~10 %
Zhao, Du & Shi (2007)	160 ($Re_x = 2$–5×10^6)	TBL flow	Random nano structures	Stain-gauge load cell	None
Daniello, Waterhouse & Rothstein (2009)	180 ($Re_H = 2$–9.5×10^3)	Channel flow	Micrograte	PIV pressure drop	~18 %
Peguero & Breuer (2009)	200 ($Re_H = 6 \times 10^3$)	Channel flow	Nanoposts	PIV	None
Woolford *et al.* (2009*b*)	100 ($Re_H = 4.8$–9.5×10^3)	Channel flow	Micrograte	PIV	~11 %
Jung & Bhushan (2010)	50 ($Re_H = 0.2$–4.6×10^3)	Channel flow	Nanoposts microposts	Pressure drop	~30 %
Current study	250	TBL flow	Micrograte	Direct reading of shifted floating surfaces	~75 %

TABLE 1. Previous experimental studies for the DR on SHPo surfaces in turbulent flows. Since different definitions of Reynolds number were used depending on the flow geometry, Re_τ are provided for fair comparison by estimating them from the Reynolds numbers provided in each reference (shown in parentheses). The result of the current study is also added.

with SHPo surface geometry. While some studies (Henoch *et al.* 2006; Daniello *et al.* 2009; Woolford *et al.* 2009*b*; Jung & Bhushan 2010) reported a substantial DR, up to ∼18 % (∼50 % if both walls of the channel are SHPo; Daniello *et al.* 2009), others (Zhao *et al.* 2007; Peguero & Breuer 2009) claimed that the slip on SHPo surfaces has negligible effects in turbulent flows. In our view, possible reasons for the inconsistency include: (i) partial or complete loss of air pockets, i.e. damaged plastron, which would underestimate the DR; (ii) a grossly thick air layer formed above the surface, i.e. overgrown plastron, which would overestimate the reduction; (iii) systematic errors caused by indirect estimation of drag based on velocity profile or pressure drop; and (iv) the effective slip being simply too small to modify the turbulence. Furthermore, most tests were limited to channel flows rather than TBL flows representing the main applications such as marine vessels and underwater structures. With all things considered, it has not been completely clear whether a SHPo surface can generate an appreciable DR in TBL flows. A systematic set of reliable experimental data is sorely missing to confirm and study SHPo DR in turbulent flows.

Challenged by the nagging doubt against the SHPo DR in TBL flows, the present study aims to experimentally confirm the DR capability of SHPo surfaces in TBL flows beyond any doubt and learn how the SHPo surface geometries affect the reduction. To solve all of the above-listed problems that possibly hindered the previous studies and ensure reliable results, we have (i,ii) designed experiments that facilitate an easy and clear monitoring of the plastron state on the sample throughout the flow tests and (iii) devised a method to read the reduction of wall-shear stress directly with little experimental uncertainties (iv) using SHPo surface geometries proven for large slip lengths. By lifting the fundamental doubt and establishing an approach to engineer the SHPo surface, we hope to convince the flow-control community to move on and investigate the hydrodynamics of SHPo surfaces more vigorously toward real-world implementations.

2. Experimental set-up

2.1. *Device for SHPo drag reduction measurement*

To resolve the first two issues raised above, which were commonly overlooked in the literature despite its importance, our experimental setup allows continuous monitoring of the plastron on the SHPo surface throughout the flow tests. To resolve the third issue, we have developed a method to measure the skin-friction DR on a SHPo surface in a direct manner with practically no bias errors. There have been long efforts to develop a robust method to measure the skin-friction drag accurately (Naughton & Sheplak 2002); however, the problem still remained. Our main strategy is to measure the variation of the skin-friction drag directly and comparatively. As illustrated in figure 1(*a*), which also defines the geometric parameters of the considered SHPo micrograte, a SHPo (i.e. slip) surface and a smooth (i.e. no-slip) surface (as a reference) are placed side-by-side in a sample, each suspended by an identical set of eight micro-flexure beams, which directs the two surfaces to displace only in one dimension. All of the elements of the 27×27 mm^2 sample were carved out from a silicon wafer by photolithographic processes in an integrated-circuit clean room (see the online supplementary data available at http://dx.doi.org/10.1017/jfm.2014.151 for details), so the two sets of flexure beams share the same processing conditions and variations during the fabrication. As a result, the two surfaces were floated by the same spring constant. This monolithic sample was flush-mounted on the upper wall of the water-tunnel test section (figure 1*b*) so that the two surfaces were always

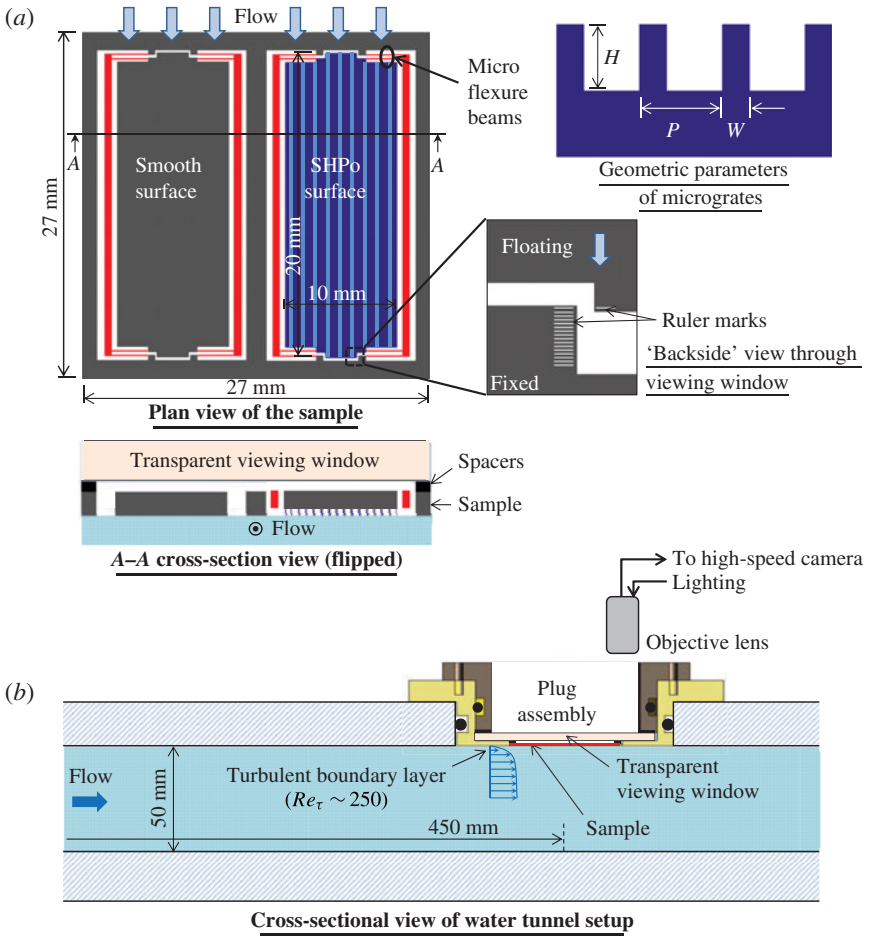

FIGURE 1. (Colour online) Schematic figures of (*a*) a sample consisting of a SHPo and a smooth surface each suspended by an identical set of flexure beam springs and (*b*) water tunnel set-up with the sample flush-mounted on the top inside wall (drawn not to scale).

under the same flows. This guarantees that any variations in both sample fabrication and flow condition are shared by the two (slip and no-slip) surfaces, so their relative shifting is solely due to the difference in the skin-friction drag acting on them.

Because a suspended surface shifts proportionally to the skin friction on it, the drag on each surface (F_s) is measured directly by reading the displacement (d) of the surface with respect to a built-in ruler (figure 1*a*) with the relation of $d = (l^3/24EI)F_s$, where l is the length of each flexure beam, E is Young's modulus (169 GPa for silicon) and I is the second moment of area for beam cross-section ($I = tw^3/12$, t is the thickness and w is the width). The nominal dimensions of the flexure beams are $l = 2500$ μm, $t = 100$ μm and $w = 15$ μm. Actual dimensions may be slightly different, w being the parameter affected by the fabrication the most and also affecting the displacement the most. Before running the flow tests, the widths of all of the flexure beams were confirmed to be within 5 % of the design. Note that, even if the measured drags are not accurate in their absolute values, their relative values are

always accurate. The side-by-side configuration of smooth and SHPo surfaces calls for consideration of potential secondary effects. First, the difference in wall shears and the resulting pressure gradient between the two surfaces may induce a secondary flow between them in spanwise direction. A rough order-of-magnitude comparison between the time scale for main (streamwise) and induced (spanwise) flows over the sample (see the online supplementary data for details) indicates that the effect of the induced flow, if any, would be very small. Second, the added flow on the SHPo surface by the spanwise inflows may increase the drag on the SHPo surface, overestimating the SHPo drag (i.e. underestimating DR). The order-of-magnitude analysis further indicates that the increase in the flow speed on the SHPo surface and the resulting drag overestimation are also negligibly small. Even without the comparative reading adopted here, microelectromechanical system (MEMS)-based sensors (using a floating element) have shown the most promise in obtaining high-resolution, instantaneous and fluctuating shear-stress measurements (Naughton & Sheplak 2002). Lastly, the fourth issue has been resolved by fabricating SHPo surfaces of grating patterns with known slip lengths, up to 33 μm, following Lee *et al.* (2008).

2.2. *SHPo surface structure*

To investigate the effect of surface geometry and explore the maximum DR obtainable under the considered flow condition, we varied the pitch (P) and gas fraction (GF) of the micrograte on SHPo surfaces. Defined as the ratio of the liquid–gas interfacial area to the overall projected area, GF is related to the width (W) and pitch (P) of the grates as $GF = (P - W)/P$ (figure 1*a*). Two sets of parametric studies were performed by varying P and GF. The first was designed to fix $P = 50$ μm and vary $W = 2.5$–35 μm to achieve $GF = 30$–$95\,\%$. The second was to fix $P = 100$ μm and vary $W = 5$–50 μm to produce $GF = 50$–$95\,\%$.

2.3. *Water-tunnel set-up*

A series of flow tests have been performed in a water tunnel, whose test section is 610 mm × 50 mm × 50 mm in the streamwise, vertical and spanwise directions, respectively, at frictional Reynolds number $Re_\tau = u_\tau \delta/\nu \sim 250$, based on the friction velocity u_τ, boundary-layer thickness δ (both obtained from the boundary-layer profile measured using laser Doppler velocimetry (LDV)), and kinematic viscosity ν, which roughly corresponds to $Re_x \sim 10^5$–10^6 common for a small unmanned underwater vehicle at cruise. The boundary-layer profile of the testing flow followed the 'log law' of turbulent flows and showed no effect of adverse pressure gradient, confirming a TBL flow over the current sample location (see figures S5 and S6 in the online supplementary data). With a spatial resolution of ∼50 μm, the LDV system used could not capture the slip velocities on the SHPo surfaces. It is noted that only micro particle image velocimetry (μPIV), whose spatial resolution is as small as $\boldsymbol{O}$ (1 μm), was able to measure discernible slips on SHPo surfaces in laminar (Joshep *et al.* 2006; Byun *et al.* 2008; Tsai *et al.* 2009) and turbulent (Daniello *et al.* 2009) flows. Special efforts were given to verify the flow is of TBL because of the relatively small Reynolds number used in this study.

To measure the instantaneous displacements of the floating surface in a turbulent flow, a high-speed camera (Vision Research Phantom V7.2) equipped with a light source and an objective lens (×20) was used at 500 frames per second (f.p.s.). The mechanical vibration generated by the pump-pipes system of the water tunnel was

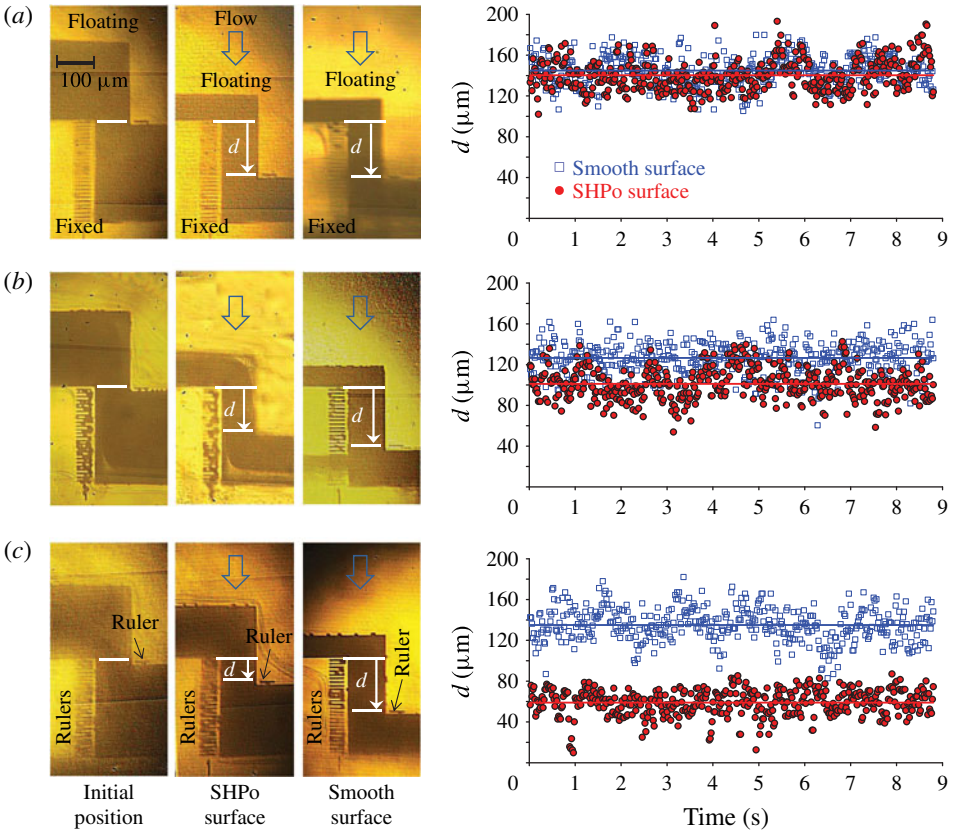

FIGURE 2. (Colour online) Displacement readings of three exemplary samples each with a smooth and a SHPo surface of: (*a*) $(P, GF) = (50\ \mu\text{m}, 30\,\%)$; (*b*) $(50\ \mu\text{m}, 60\,\%)$; (*c*) $(50\ \mu\text{m}, 90\,\%)$. The optical pictures, corresponding to the magnified drawing entitled 'backside view through viewing window' in figure 1, are among the millions of images captured during flow tests. Compared with the initial positions (first column), the SHPo (second column) and smooth (third column) surfaces were displaced along the flow direction (denoted as open arrows) against the fixed surfaces by d when TBL flows over the sample. The temporal displacements of the SHPo (●, shown in red online) and smooth (□, shown in blue online) surfaces are shown in the corresponding graphs (fourth column). The solid lines denote the time-averaged displacements of the floating surfaces. Note that the current measurement method captures the fluctuating nature of the turbulent skin-friction drag.

first confirmed too small to affect the measurement. After each measurement, it was confirmed that the floating surfaces return to the initial positions, to make sure there was no permanent effect of the flows on the surfaces. The 50 f.p.s. data points (see figure 2) have been reduced from the raw 500 f.p.s. images. Recorded displacements were analyzed to obtain the statistical data (time-averaged displacement and root-mean-square (r.m.s.) fluctuation) with ImageJ software. Since the natural frequency of the current floating surface is only ~40 Hz, the fluctuating characteristics of measured displacement (i.e. drag) is originated from the flow condition (i.e. turbulence).

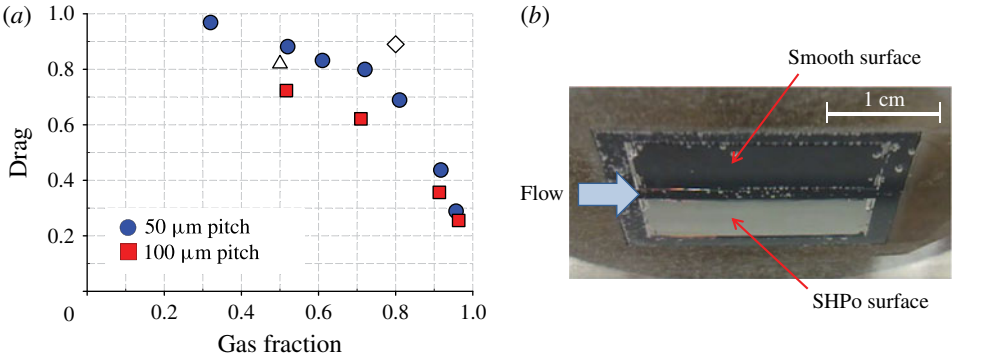

FIGURE 3. (Colour online) Effect of SHPo surface geometry in TBL flow ($Re_\tau \sim 250$). (*a*) Variation of normalized drag with gas fraction (*GF*) for pitches of 50 μm (●, shown in blue online) and 100 μm (■, shown in red online). Two available results of micrograte SHPo surfaces, although measured in turbulent channel flows, are included for comparison: △, 60 μm pitch and 50 % *GF* ($Re_\tau \sim 180$) (Daniello *et al.* 2009); ◊, 40 μm pitch and 80 % *GF* ($Re_\tau \sim 100$) (Woolford *et al.* 2009*b*). (*b*) Picture of a sample during flow test. Collapse (even one trench) or overgrowth (e.g. merging of neighboring air pockets) of the plastron was readily detectable; if so (rare), the test was aborted. The SHPo surface in this sample produced the largest reduction rate (∼75 %) in the current study.

3. Results and discussion

3.1. *Turbulent DR on SHPo surfaces*

Shown in figure 2 are the pictures of instantaneous displacements captured for three exemplary samples, i.e. three pairs of SHPo and smooth surfaces, along with the temporal variation of displacement measured for each corresponding sample. Depending on the surface geometry, the SHPo surface may show a distinctively smaller displacement (i.e. smaller drag) than the smooth surface, while the difference indicates the DR. As shown in figure 2(*a*), the SHPo surface of 50 μm pitch and 30 % *GF*, which would produce a relatively small surface slip (∼2 μm) (Lauga & Stone 2003), displaces (i.e. drags) nearly as much as the smooth surface, indicating little DR. However, the SHPo surfaces of higher *GF* with larger slips (∼10 and 33 μm) (Lauga & Stone 2003) displace distinctively less than their smooth counterparts (figure 2*b*,*c*), clearly indicating a DR. These results provide strong evidence of DR by SHPo surfaces in a TBL flow with a clear trend by their geometric parameters for the first time. Considering many other unsuccessful attempts, the success additionally emphasizes the importance of ensuring the existence of plastron and properly designed and fabricated surface profiles for turbulent DR. Only after microscopic details of the SHPo structures had been refined further from those developed for the laminar flows (Lee *et al.* 2008; Lee & Kim 2009), was a stable air–water interface guaranteed and a reliable DR obtained in the present TBL flow.

For each sample, the time-averaged displacement of the SHPo surface was normalized to that of the smooth surface in order to produce a normalized SHPo drag rate without a bias error. By collecting the data of all of the samples, figure 3(*a*) reveals how *P* and *GF* of the micrograte affect the SHPo DR in the tested TBL flow. The *GF* values plotted in figure 3(*a*) are of the fabricated samples, slightly different from the nominal values of the design. For both 50 and 100 μm pitch, the drag on

SHPo surfaces decreases with GF, reaching as small as 25 % at $GF = 95$ %. This DR of 75 % is significantly larger than the previously largest DR of ∼18 % on a SHPo surface (Daniello *et al.* 2009). The result is not surprising, considering the 95 % GF of the current surface is nearly twice of theirs 50 % GF. Furthermore, figure 3(*a*) shows that 100 μm pitch reduces the drag more than 50 μm pitch does for a given GF. The trend of a smaller drag on a larger pitch is somewhat expected from the larger slip confirmed in the laminar flow (Choi *et al.* 2006; Lee *et al.* 2008) and the smaller drag found in a turbulent channel flow (Daniello *et al.* 2009). Interestingly, the effect of pitch is shown to diminish when GF is very large. At $GF \sim 50$ %, for example, the DR is more than doubled when the pitch increases from 50 to 100 μm. At $GF > 90$ %, however, the DR only slightly increases with the pitch; instead the GF plays a bigger role. Currently it is not clear which parameter dominates in determining the DR. Contributions of various parameters will be discussed as a scaling issue in § 3.3.

3.2. *Comparison with previous studies*

Examining table 1, one may find that some SHPo surfaces with longitudinal grates in micro-scale reported a DR while no SHPo surface with nano-scale grates or random structures produced any positive results. We believe the nano-scale slip lengths on nano-scale grates were too small to be effective in the tested flow systems, as they were measurable only in a micro-scale channel (Choi *et al.* 2006), and the spanwise slip on random structures negated the DR created by the streamwise slip (Hahn, Je & Choi 2002; Min & Kim 2004; Busse & Sandham 2012). Based on this observation, we will compare the present results only with the previous works on micro-scale grates. In figure 3(*a*), two experimental data (two hollow symbols) from Daniello *et al.* (2009) and Woolford *et al.* (2009*b*) are added for comparison. Since DR was more than doubled when both the upper and lower channel walls were SHPo instead of only one wall (Daniello *et al.* 2009), indicating the confinement effect of channel flows, the result with one SHPo wall is plotted for a fair comparison. Although they were performed in channel flows, their Reynolds numbers ($Re_\tau \sim 180$ and 100, estimated from the provided data (Daniello *et al.* 2009; Woolford *et al.* 2009*b*)) were similar to the current study in a TBL flow ($Re_\tau \sim 250$). Considering their pitches and GF, the 11 % (◇ in figure 3*a*) (Woolford *et al.* 2009*b*) and 18 % DR (△ in figure 3*a*) (Daniello *et al.* 2009) look reasonable when compared with the current data.

The above comparison also prompted us to speculate how the Reynolds number affects the turbulent DR by ignoring the differences in experimental details. In figure 3(*a*), the DR at $Re_\tau = 100$ (Woolford *et al.* 2009*b*) and $Re_\tau = 180$ (Daniello *et al.* 2009) appear less and more, respectively, than the current DR at $Re_\tau = 250$, showing no clear trend. Furthermore, Daniello *et al.* (2009) reported the DR over a range of $Re_\tau \sim$ 100–300 (roughly converted from the Re_H range reported), but the data scattered too much to reveal any trend. This is in contrast to the positive trend (i.e. more DR at higher Re) predicted by numerical studies (Fukagata *et al.* 2006; Busse & Sandham 2012; Park *et al.* 2013). The above observation indicates that one would need a much wider range of Reynolds numbers than the reported to experimentally study the effect of Reynolds number on turbulent DR.

3.3. *Scaling*

Figure 3(*a*) indicates that as GF increases the drag decreases, ultimately approaching a near-zero drag at $GF = 100$ %. The drag decreases very fast after the GF becomes

very high (e.g. over 90 %), closely resembling the *GF* versus the inverse of slip length in laminar flows (Lee *et al.* 2008). The maximum DR achievable in turbulent channel flows has been explained by the effective slip length in wall units ($\lambda^+ = \lambda u_\tau/\nu$) through numerical simulations (Fukagata *et al.* 2006; Busse & Sandham 2012; Park *et al.* 2013). They showed that to obtain a substantial DR, the slip length should be comparable to the viscous sublayer thickness, i.e. $\lambda^+ \sim 5$, and that the DR would saturate if the slip length reaches a very large value, $\lambda^+ = \boldsymbol{O}(10^2)$. Main idea for this scaling is that unlike in laminar flows where the DR is a direct consequence of slip, in turbulent flows both direct (slip) and indirect (suppression of near-wall turbulence structures) effects are likely to contribute to DR (Hahn *et al.* 2002; Min & Kim 2004; Fukagata *et al.* 2006; Busse & Sandham 2012; Park *et al.* 2013). On the other hand, others claimed that the spacing (k) of SHPo surface features (e.g. $k = P - W$ in case of micrograte) is more important than the *GF*, based on their numerical simulations (Martell *et al.* 2010) and experiment (Daniello *et al.* 2009) on turbulent channel flows. It was claimed that to impact the turbulent flow, the spacing in wall unit should reach the thickness of the viscous sublayer, i.e. $k^+ \sim 5$, and that as the Reynolds number increases, the DR would approach a limit, which is identical to the *GF* value (Daniello *et al.* 2009). For the present SHPo surface geometries, the spacing of the microgrates is $k^+ = 0.3$–2 in wall units, which is in a similar range as Daniello *et al.* (2009). However, the cases of 50 μm pitch with 90 % and 95 % *GF* ($k^+ = 0.91$ and 0.97, respectively) showed much larger DR than the cases of 100 μm pitch with 50 % and 70 % *GF* ($k^+ = 1$ and 1.4, respectively), indicating that the spacing alone is not a proper parameter to characterize the DR and we need to consider the effects from other parameters as well. Recently, Park *et al.* (2013) revealed, from a direct numerical simulation on turbulent channel flows with SHPo walls, that the amount of DR for different gratings and Reynolds numbers was well scaled with λ^+, i.e. the skin-friction drag decreased with increasing slip length λ^+. The effect of increasing λ^+ was saturated at $\lambda^+ > 40$, indicating that high skin friction in wall-bounded turbulent flows are largely attributed to the turbulence structures which are primarily found in the buffer layer ($y^+ = 10$–50) (Kim 2011). With the present data, a clear relationship could not be established between the turbulent DR and the effective slip length λ estimated by the laminar analytical solution (Lauga & Stone 2003), unlike the laminar case where DR could be determined from λ in comparison with the characteristic length (e.g. channel height) (Choi *et al.* 2006). The difference is evident as the DR measured in the present study is much larger than what would be estimated from the laminar analytical solution. This scaling issue is very important to design SHPo surfaces for very high-Reynolds-number flows and needs to be confirmed experimentally in future studies.

3.4. *Comments on the plastron stability*

All of the present data were obtained with the SHPo surfaces maintaining the plastron as designed; all of the air pockets were confirmed to sustain without any loss or merging for hours, much longer than needed to complete testing a sample (∼30 min). Noting that there is almost no mention in the literature of the state of the plastron despite its frailty during the flow tests and suspecting such an oversight was the main reason for the inconsistent results in many SHPo DR studies, we designed the experimental set-up to allow easy monitoring of the plastron state with naked eyes. The picture of figure 3(*b*) shows that the wetting condition of the sample surfaces can be continuously monitored during the flow test. The SHPo surface shows

a silvery color due to the different refraction index of the air in the plastron while the smooth surface has a dark color. The sample pictured in figure 3(*b*) had a SHPo surface with the largest pitch and the highest *GF* ($P = 100$ μm and $GF = 95\,\%$). Although a larger pitch or higher *GF* would reduce the drag even more according to the trend (figure 3*a*), the plastron on such SHPo surfaces were found to become unstable in the given TBL flow, resulting in the loss of air (i.e. wetting). The plastron on SHPo surfaces was found to be less stable at higher *GF*, following a similar trend established and explained for laminar flows (Lee & Kim 2009). However, our current knowledge is not mature enough to pinpoint why the plastron is more susceptible to breakdown in turbulent flows compared with laminar flows, other than suspecting several characteristics of turbulent flows such as pressure fluctuation, large shear and shear rate at the wall, large skin-friction drag, and intermittency. In comparison, in well-controlled laminar flows (Lee *et al.* 2008), we were able to maintain a plastron on similar surfaces of larger P and higher *GF*, up to $P = 200$ μm and $GF = 98\,\%$. Since maintaining the plastron is more critical for real-world applications, where the static and/or dynamic hydrodynamic conditions are harsher under very high Reynolds numbers ($Re_\tau \sim 10^5$), they may require a relatively small pitch for a more robust plastron. Although only one Reynolds number has been used, the current results support the expectation that the DR can remain substantial even on small pitches at very high Reynolds numbers (Min & Kim 2004; Fukagata *et al.* 2006; Busse & Sandham 2012; Park *et al.* 2013). The decreasing DR on the decreasing pitch would be countered by decreasing viscous length scale (i.e. viscous sublayer thickness) of an increasing Reynolds number. While the overall trend is encouraging, more research is needed to quantify the trend and identify limitations.

4. Conclusions

Assisted by a direct and comparative measurement of skin-friction drag and a genuine plastron in place during all flow tests, we have positively confirmed that the SHPo surfaces reduce the skin-friction drag in turbulent flows. Within the considered ranges, DR as large as ∼75 % has been achieved and a clear trend of DR found as a function of surface grating parameters. The present result is exciting because of the significant benefits expected. For instance, in maritime transportation the skin friction contributes to 60–70 % of the total drag on a cargo ship and 80 % on a tanker (Fukuda *et al.* 2000). Considering that shipping alone accounts for 8.5 % of the global oil supply (Winkler 2008) and 3.3 % of CO_2 emissions (Qi & Song 2012), even a mild DR has a global impact for energy saving and greenhouse gas reduction. With the DR on SHPo surfaces in TBL flows confirmed, one can next perform systematic studies with various SHPo surfaces in a wide range of hydrodynamic flows. As the basic design knowledge is now acquired, time is ripe to focus on more practical issues, such as the longevity (stability) of plastron in the flow conditions of large vessels (e.g. $Re_\tau \sim 10^5$); the development of a low-cost mass production for the SHPo surfaces; and the methodology of deploying SHPo surfaces in real-world applications.

Acknowledgements

This work has been supported by the ONR Grant (No. N000141110503) and NSF Grant (No. 1336966). The authors thank John Kim and Hyunwook Park for fruitful discussions, MSE Inc. (Pasadena, USA) for providing velocity profiles of TBL flows, and Ryan Freeman for help with the manuscript.

Supplementary data

Supplementary data are available at http://dx.doi.org/10.1017/jfm.2014.151.

REFERENCES

BOCQUET, L. & LAUGA, E. 2011 A smooth future? *Nat. Mater.* **10**, 334–337.

BUSSE, A. & SANDHAM, N. D. 2012 Influence of an anisotropic slip-length boundary condition on turbulent channel flow. *Phys. Fluids* **24**, 055111.

BYUN, D., KIM, J., KO, H. S. & PARK, H. C. 2008 Direct measurement of slip flows in superhydrophobic microchannels with transverse grooves. *Phys. Fluids* **20**, 113601.

CECCIO, S. L. 2010 Friction drag reduction of external flows with bubble and gas injection. *Annu. Rev. Fluid Mech.* **42**, 183–203.

CHOI, C.-H. & KIM, C.-J. 2006 Large slip of aqueous liquid flow over a nanoengineered superhydrophobic surface. *Phys. Rev. Lett.* **96**, 066001.

CHOI, C.-H., ULMANELLA, U., KIM, J., HO, C.-M. & KIM, C.-J. 2006 Effective slip and friction reduction in nanograted superhydrophobic microchannels. *Phys. Fluids* **18**, 087105.

DANIELLO, R. J., WATERHOUSE, N. E. & ROTHSTEIN, J. P. 2009 Drag reduction in turbulent flows over superhydrophobic surfaces. *Phys. Fluids* **21**, 085103.

EMAMI, B., HEMEDA, A. A., AMREI, M. M., LUZAR, A., GAD-EL-HAK, M. & TAFRESHI, H. V. 2013 Predicting longevity of submerged superhydrophobic surfaces with parallel grooves. *Phys. Fluids* **25**, 062108.

FUKAGATA, K., KASAGI, N. & KOUMOUTSAKOS, P. 2006 A theoretical prediction of friction drag reduction in turbulent flow by superhydrophobic surfaces. *Phys. Fluids* **18**, 051703.

FUKUDA, K., TOKUNAGA, J., NOBUNAGA, T., NAKATANI, T., IWASAKI, T. & KUNITAKE, Y. 2000 Frictional drag reduction with air lubricant over a super-water-repellent surface. *J. Mar. Sci. Technol.* **5**, 123–130.

HAHN, S., JE, J. & CHOI, H. 2002 Direct numerical simulation of turbulent channel flow with permeable walls. *J. Fluid Mech.* **450**, 259–285.

HASEGAWA, Y., FROHNAPFEL, B. & KASAGI, N. 2011 Effects of spatially varying slip length on friction drag reduction in wall turbulence. *J. Phys.: Conf. Ser.* **318**, 022028.

HENOCH, C., KRUPENKIN, T. N., KOLODNER, P., TAYLOR, J. A., HODES, M. S., LYONS, A. M., PEGUERO, C. & BREUER, K. 2006 Turbulent drag reduction using superhydrophobic surfaces, *AIAA Paper 2006-3192*.

JEFFS, K., MAYNES, D. & WEBB, B. W. 2010 Prediction of turbulent channel flow with superhydrophobic walls consisting of micro-ribs and cavities oriented parallel to the flow direction. *Intl J. Heat Mass Transfer* **53**, 786–796.

JIMÉNEZ, J. 2004 Turbulent flows over rough walls. *Annu. Rev. Fluid Mech.* **36**, 173–196.

JOSHEP, P., COTTIN-BIZONNE, C., BENOÎT, J.-M., YBERT, C., JOURNET, C., TABELING, P. & BOCQUET, L. 2006 Slippage of water past superhyrophobic carbon nanotube forests in microchannels. *Phys. Rev. Lett.* **97**, 156104.

JUNG, Y. C. & BHUSHAN, B. 2010 Biomimetic structures for fluid drag reduction in laminar and turbulent flows. *J. Phys.: Condens. Matter* **22**, 035104.

KIM, J. 2011 Physics and control of wall turbulence for drag reduction. *Phil. Trans. R. Soc.* A **369**, 1396–1411.

LAUGA, E. & STONE, H. 2003 Effective slip in pressure-driven Stokes flow. *J. Fluid Mech.* **489**, 55–77.

LAY, K. A., RYO, Y., SIMO, M., PERLIN, M. & CECCIO, S. L. 2010 Partial cavity drag reduction at high Reynolds numbers. *J. Ship Res.* **54**, 109–119.

LEE, C., CHOI, C.-H. & KIM, C.-J. 2008 Structured surfaces for a giant liquid slip. *Phys. Rev. Lett.* **101**, 064510.

LEE, C. & KIM, C.-J. 2009 Maximizing the giant liquid slip on superhydrophobic microstructures by nanostructuring their sidewalls. *Langmuir* **25**, 12812–12818.

LEE, C. & KIM, C.-J. 2011 Underwater restoration and retention of gases on superhydrophobic surfaces for drag reduction. *Phys. Rev. Lett.* **106**, 014502.

LEE, C. & KIM, C.-J. 2012 Wetting and active dewetting processes of hierarchically constructed superhydrophobic surfaces fully immersed in water. *J. Microelectromech. Syst.* **21**, 712–720.

MARTELL, M. B., PEROT, J. B. & ROTHSTEIN, J. P. 2009 Direct numerical simulations of turbulent flows over superhydrophobic surfaces. *J. Fluid Mech.* **620**, 31–41.

MARTELL, M. B., ROTHSTEIN, J. P. & PEROT, J. B. 2010 An analysis of superhydrophobic turbulent drag reduction mechanisms using direct numerical simulation. *Phys. Fluids* **22**, 065102.

MAYNES, D., JEFFS, K., WOOLFORD, B. & WEBB, B. W. 2007 Laminar flow in a microchannel with hydrophobic surface patterned microribs oriented parallel to the flow direction. *Phys. Fluids* **19**, 093603.

MIN, T. & KIM, J. 2004 Effects of hydrophobic surface on skin-friction drag. *Phys. Fluids* **16**, L55–L58.

NAUGHTON, J. W. & SHEPLAK, M. 2002 Modern developments in shear-stress measurement. *Prog. Aerosp. Sci.* **38**, 515–570.

OU, J., PEROT, B. & ROTHSTEIN, J. P. 2004 Laminar drag reduction in microchannels using ultrahydrophobic surfaces. *Phys. Fluids* **16**, 4635–4643.

PARK, H., PARK, H. & KIM, J. 2013 A numerical study of the effects of superhydrophobic surface on skin-friction drag in turbulent channel flow. *Phys. Fluids* **25**, 110815.

PEGUERO, C. & BREUER, K. 2009 On drag reduction in turbulent channel flow over superhydrophobic surfaces. In *Advances in Turbulence XII* (ed. B. Eckhardt), pp. 233–236. Springer.

QI, X. & SONG, D.-P. 2012 Minimizing fuel emissions by optimizing vessel schedules in liner shipping with uncertain port times. *Transp. Res.* E **48**, 863–880.

ROTHSTEIN, J. P. 2010 Slip on superhydrophobic surfaces. *Annu. Rev. Fluid Mech.* **42**, 89–109.

SAMAHA, M. A., TAFRESHI, H. V. & GAD-EL-HAK, M. 2012*a* Influence of flow on longevity of superhydrophobic coatings. *Langmuir* **28**, 9759–9766.

SAMAHA, M. A., TAFRESHI, H. V. & GAD-EL-HAK, M. 2012*b* Superhydrophobic surfaces: from the lotus leaf to the submarine. *C.R. Méc.* **340**, 18–34.

TSAI, P., PETERS, A. M., PIRAT, C., WESSLING, M., LAMMERTINK, R. G. H. & LOHSE, D. 2009 Quantifying effective slip length over micro patterned hydrophobic surfaces. *Phys. Fluids* **21**, 112002.

WALSH, M. J. 1982 Turbulent boundary layer drag reduction using riblets *AIAA Paper 1982-0169*.

WINKLER, J. P. 2008 Shipping wasting 4.37 million barrels of oil a day. Reuters Press Release, http://www.reuters.com/article/2008/06/24/idUS82323+24-Jun-2008+BW20080624.

WOOLFORD, B., MAYNES, D. & WEBB, B. W. 2009*a* Liquid flow through microchannels with grooved walls under wetting and superhydrophobic conditions. *Microfluid. Nanofluid.* **7**, 121–135.

WOOLFORD, B., PRINCE, J., MAYNES, D. & WEBB, B. W. 2009*b* Particle image velocimetry characterization of turbulent channel flow with rib patterned superhydrophobic walls. *Phys. Fluids* **21**, 085106.

ZHAO, J., DU, X. & SHI, X. 2007 Experimental research on friction–reduction with super-hydrophobic surfaces. *J. Mar. Sci. Appl.* **6**, 58–61.